KSME International Journal, Vol. 16 No. 7, pp. 919~926, 2002

A Study on μBGA Solder Joints Reliability Using Lead-free Solder Materials

Young-Eui Shin*, Jun-Hwan Lee, Young-Wook Koh, Chong-Won Lee
Department of Mechanical Engineering, Chung-Ang University, Seoul 156-756, Korea
Jun-Ho Yun
Department of Automobiles, Yeojoo Institute of Technology University, Seoul 156-756, Korea
Seung-Boo Jung
Department of Metallurgical Engineering, Sungkyunkwan University, Kyunggi-do 440-746, Korea

In this study, the numerical prediction of the thermal fatigue life of a μBGA (Micro Ball Grid Array) solder joint was focused. Numerical method was performed using the three-dimensional finite element analysis for various solder alloys such as Sn-37%Pb, Sn-3.5%Ag, Sn-3.5%Ag-0.7%Cu and Sn-3.5%Ag-3%In-0.5%Bi during a given thermal cycling. Strain values obtained by the result of mechanical fatigue tests for solder alloys, were used to predict the solder joint fatigue life using the Coffin-Manson equation. The numerical results showed that Sn-3.5%Ag with the 50-degree ball shape geometry had the longest thermal fatigue life in low cycle fatigue. A practical correlation for the prediction of the thermal fatigue life was also suggested by using the dimensionless variable γ. Additionally Sn-3.5Ag-0.75Cu and Sn-2.0Ag-0.5Cu-2.0Bi were applied to $6\times8\mu$BGA obtained from the 63Sn-37Pb Solder. This $6\times8\mu$BGA were tested at different aging conditions at 130℃, 150℃, 170℃ for 300, 600 and 900 hours. Thickness of the intermetallic compound layer was measured for each condition and the activation energy for their growth was computed. The fracture surfaces were analyzed using SEM (Scanning Electron Microscope) with EDS (Energy Dispersive Spectroscopy).

Key Words : Thermal Fatigue Life, Finite Element Method, Lead-Free Solder, Intermetallic Compound, Solder Joint, Micro Ball Grid Array

1. Introduction

Rapid development in the mobile communication equipments and the modern electronic devices requires high performance, miniaturization and lightweight. The packaging technology for electronic devices has been developed from the QFP (Quad Flat Package) and BGA (Ball Grid Array) toward the CSP (Chip Scale Package) (Yao et al. 1999; Amagai 1999) and Flip Chip (Partridge et al. 1998). Technical development in this area is very important to achieve improved designs. μBGA (Micro Ball Grid Array), a kind of CSP, used in small electronic equipments such as mobile phones has a ball size of 0.3~0.35mm and a fine pitch of 0.5~0.75mm. μBGA has more complex structure and higher chip size ratio in package compared with the common BGAs. Therefore, a proper estimation method for the thermal fatigue life of the μBGA is required for the micro solder joint design. Since the usage of Sn-Pb

* Corresponding Author,
E-mail : shinyoun@cau.ac.kr
TEL : +82-2-820-5315; **FAX** : +82-2-814-9476
Department of Mechanical Engineering, Chung-Ang University, Seoul 156-756, Korea. (Manuscript **Received** December 18, 2001; **Revised** April 38, 2002)

Copyright (C) 2003 NuriMedia Co., Ltd.

solder alloys will be restricted for the electronic equipments due to environmental problems, a study on the Pb-free solders becomes an important research topic.

In this paper, the life estimation of the μBGA solder joint with Pb-free solders as well as Sn-37Pb was studied. To study the effect of the solder shape on the life, three different shapes for four different solder alloys were analyzed. Stress and strain results obtained from FEA were used to predict the thermal fatigue life through the Coffin-Manson equation and available data (Oguchi et al. 1998; Kariya et al. 1998). Finally, a new equation for thermal fatigue life was suggested using the dimensionless variable γ which is a function of temperature variables.

2. Experimental Analysis and Finite Element Analysis

2.1 Aging test

$6\times8\mu$BGA used in aging is longer than chips by 0.5mm and the pitch between copper pads is 0.75mm, which is a type of Chip Size Package (CSP). Nubin, a sort of elastomer, was used as a stress relief material. Additionally, lead-free solder balls manufactured from Senju Metal Industry having the diameter of 0.35mm were used, and their chemical compositions were Sn-3.5Ag-0.75Cu and Sn-2.0Ag-0.5Cu-2.0Bi. RMA SR-12 from Alpha Metal Industry was used as a flux, and the reflow machine (infrared rays type and hot air heating reflow) was used for soldering. Overall reflow time was 5 minutes, and the conveyer speed was 0.55m/min. The maximum temperatures for 63Sn-37Pb and Sn-3.5Ag solders were 230℃ and 260℃, respectively. The time for the liquid state was 60 seconds. Bonding tester of Rheseas PRT-1000, was used for shear stress test. The dipping specimen was 0.2mm/s and height was 5mm. Shear stresses were measured from three specimens and each specimen was tested for 24 balls. The average values were calculated excluding maximum and minimum values.

2.2 Numerical simulation by FEA

To assess a long term reliability of the μBGA solder joint, the most important criterion is the failure by thermal fatigue. This is observed as the result of the thermal expansion of each component caused by the heating up and cooling down of the chip or by the temperature change of the circumstance. As the result, a thermal stress is concentrated on the micro-joining interface continuously and the solder joint will cause the thermal fatigue fracture. At that time, the difference of total CTE (Coefficient of Thermal Expansion) for PCB and package should be considered regarding thermal displacement caused by the temperature change. The thermal fatigue failure usaally occurs in the upper part of the solder joint as shown in Fig. 1. Because the solder joint has low yield stress and results easily in an unrecoverable plastic deformation, its material characteristics is independent of the time. Additionally, thermal fatigue of the solder joint is affected by formation change of material. So that the failure mechanism becomes complicated. While strain and stress that occur in solder joint are complex about each axis, they can be expressed by single axis equivalent strain and stress using von Mises equation.

$$\sigma_{eq}=\sqrt{(1/2)}\,[(\sigma_1-\sigma_2)^2+(\sigma_2-\sigma_3)^2+(\sigma_3-\sigma_1)^2]^{1/2} \quad (1)$$

$$\varepsilon_{eq}=\sqrt{(1/2)}\,[(\varepsilon_1-\varepsilon_2)^2+(\varepsilon_2-\varepsilon_3)^2+(\varepsilon_3-\varepsilon_1)^2]^{1/2} \quad (2)$$

where, $\sigma_i(i=1, 2, 3)$: principal stress, $\varepsilon_i(i=1, 2, 3)$: principal strain

The equivalent strain and stress values can be found by temperature change from the equations. Total equivalent strain from FEA result is defined as :

$$\varepsilon_t=\varepsilon_{el}+\varepsilon_{in} \quad (3)$$

where, ε_t: total equivalent strain, ε_{el}: elastic strain, ε_{in}: non-elastic strain.

The Coffin-Manson equation (Coffin et al. 1954) and the modified Coffin-Manson equations (Engelmeier 1983; Lee et al. 2000) were used to observe the relationship between equivalent plastic strain and fatigue life.

$$\Delta\varepsilon_p * N_f^{\alpha}=C \quad (4)$$

For the thermal stress analysis of the solder joint, ANSYS was used. The solder joint between 6×8 μBGA and PCB was considered. Since the

Copyright (C) 2003 NuriMedia Co., Ltd.

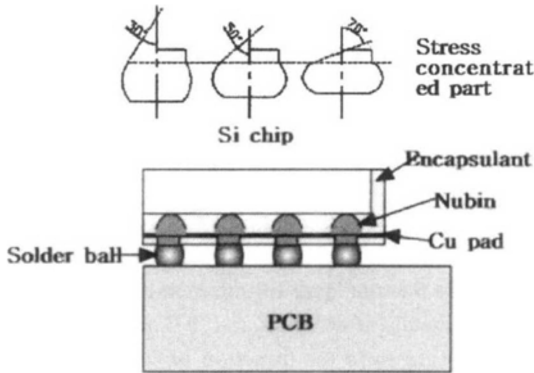

Fig. 1 Symmetric diagram of μBGA and solder ball

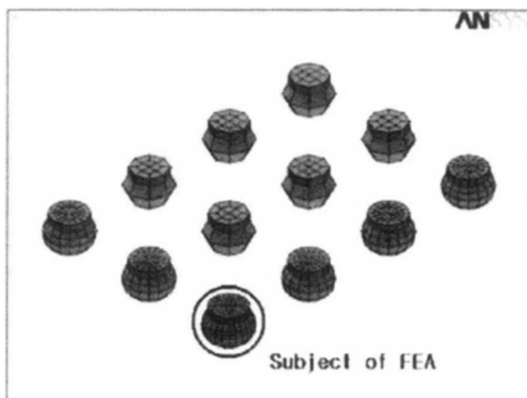

Fig. 2 Finite Element Model of μBGA Solder Joint

module was symmetric, a quarter of the whole part was selected for the modeling. Considering the influences in stress and life, the model was simplified with 6 different materials which were Si chip, encapsulant, Cu-pad, Polyimid film, Nubbin (Low modulus elastomer material) and FR-4 PCB. Figure 1 shows the schematic diagram of μBGA and Fig. 2 shows the μBGA after modeling. The solder joint in Fig. 2 with the fatigue failure caused by the stress concentration was frequently observed (from thermal fatigue experiments). For FEA modeling, 8 node thermal, structural and viscosity elements were used.

All materials except solder alloys were assumed to be isotropic, linear elastic and bi-linear kinematics hardening at yielding stress as shown in Fig. 3 (Lau et al. 1998 ; Shin et al. 1999). The relationship between the yielding stress and temperature was assumed to be inverse-linear.

Table 1 Mechanical fatigue constant of various solder materials

	Sn-37Pb	Sn-3.5Ag	Sn-3.5Ag-0.7Cu	Sn-3.5Ag-3In-0.5Bi
C	0.24	0.9	0.46	0.60
α	0.49	0.5	0.43	0.51

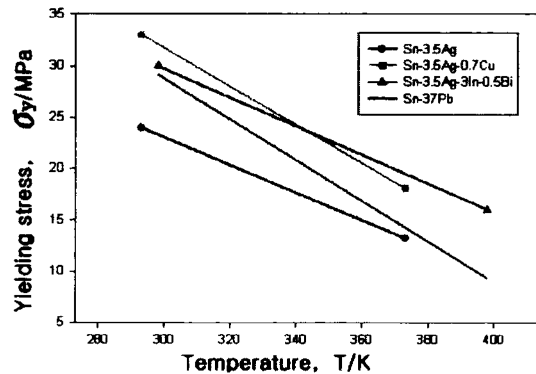

Fig. 3 Correlaton of yielding stress with temperature (Lau et al. 1998 ; Shin et al. 1999)

Table 1 (Kariya et al. 1998 ; Shin et al. 1999) represents the fatigue constants of different solder alloys. Displacement in the axial direction at a quarter cutting surface was constrained by the boundary condition. For load conditions, thermal cycles were set to have a uniform temperature distribution at all nodes. Reference temperature for determining the thermal expansion was set to 293K. Three whole cycles were applied to get a stable strain hysteresis loop due to the non-linearity of the solder and to minimize the transient ratcheting and shakedown effects.

3. Results and Discussions

3.1 Metallurgical characteristics

In order to investigate the change of mechanical properties of micro-structure on bonding, Sn-3.5Ag-0.75Cu and Sn-2.0Ag-0.5Cu-2.0Bi were tested for shear stress after aging, and the results were compared with 63Sn-37Pb solder. Two lead-free solders showed higher strength under aging. Lead free-solder added with element group four Bi was confirmed to have higher strength.

Figure 4 shows the surface of lead-free solder

Copyright (C) 2003 NuriMedia Co., Ltd.

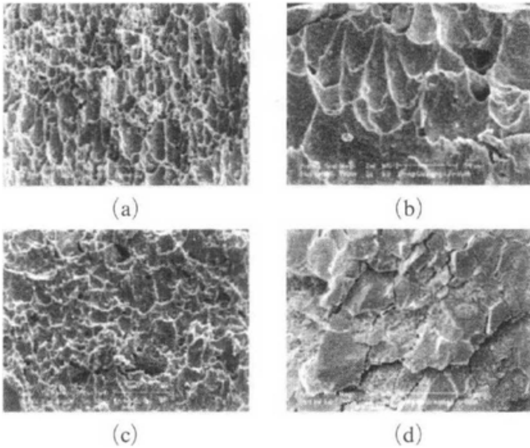

(a) (b)

(c) (d)

Fig. 4 Fig. 4 Fracture surface of Sn-3.5Ag-0.75Cu (a: no aging, b: aging 170℃, 900h) and Sn-2.0Ag-0.5Cu-2.0Bi (c: no aging, d: aging 170℃, 900h)

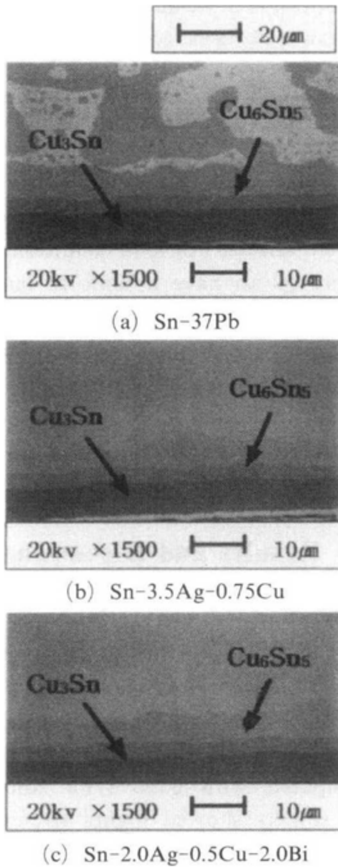

(a) Sn-37Pb

(b) Sn-3.5Ag-0.75Cu

(c) Sn-2.0Ag-0.5Cu-2.0Bi

Fig. 5 Two phase of intermetallic compound layer with solder alloys

after shear stress test at 170℃ with 900 hours aging. As the intermetallic compound grew by aging, the strength were decreased. SEM and EDX were used to observe the intermetallic compound layer on the specimen surface. Through the EDX, only η phase was occurred at the beginning of aging; however, ε phase was observed after aging.

Figure 5 is the layer of intermetallic compound of two metals after aging at 170℃ for 900 hours. η phase grows to the direction of solder between solder and cuper pad because Cu has faster speed of diffusion. ε phase was not observed at the initial bonding because ε phase was more difficult to be nucleated than η phase.

3.2 Prediction of thermal fatigue life

The computed average elastic-plastic strain is listed in Table 2. Results showed that the plastic strain was increased in the order as Sn-37Pb < Sn-3.5Ag-3In-0.5Bi < Sn-3.5Ag-0.7Cu < Sn-3.5 Ag at the lower temperature range. Howerer, at the higher temperature range, the tendency changed to be Sn-37Pb < Sn-3.5Ag-0.7Cu < Sn-3.5Ag-3In-0.5Bi < Sn-3.5Ag. Elastic deformation was relatively small as compared to the plastic deformation except for the temperature range of 233K ~ 373K. This implies that it is rational to consider only the plastic deformation for estimation of the thermal fatigue life.

The inelastic strain, which depends on the frequency, can be classified into plastic and creep strain. Since the results of thermal fatigue life (Kariya et al. 1998; Engelmeier 1983; Maeda 1999) are mainly dependent on the plastic and creep strain, the creep strain needs to be applied especially when the strain rate is under 0.025Hz. When the strain rate is over 0.25Hz, the plastic strain need to be taken into account for the solder joint. In case that the total strain rate is larger than the maximum creep strain, the plastic strain plays the major role in solder joint deformation. Therefore, in this study, it was assumed that the inelastic strain occurred in the solder joint was only due to the plastic strain. Plastic strains for different temperatures and materials were used to estimate the thermal fatigue life and to predict the

Copyright (C) 2003 NuriMedia Co., Ltd.

Table 2 Mean elastic-plastic strain amplitude in various conditions

Tcycle(K)			Sn-37Pb	Sn-3.5Ag	Sn-3.5Ag-0.7Cu	Sn-3.5Ag-3In-0.5Bi
$\Delta\varepsilon_{el}$	293~373		0.000592	0.000267	0.000347	0.000303
	253	30°	0.000799	0.000248	0.000427	0.000317
	~	50°	0.000599	0.000209	0.000321	0.000257
	373	70°	0.000718	0.000332	0.000372	0.000383
	233~393		0.000915	0.000381	0.000489	0.000483
$\Delta\varepsilon_{pl}$	293~373		0.001466	0.003626	0.003713	0.00848
	253	30°	0.003957	0.007859	0.008242	0.004778
	~	50°	0.003030	0.004945	0.004996	0.002363
	373	70°	0.007546	0.008768	0.008377	0.005347
	233~393		0.006745	0.015806	0.014786	0.014668

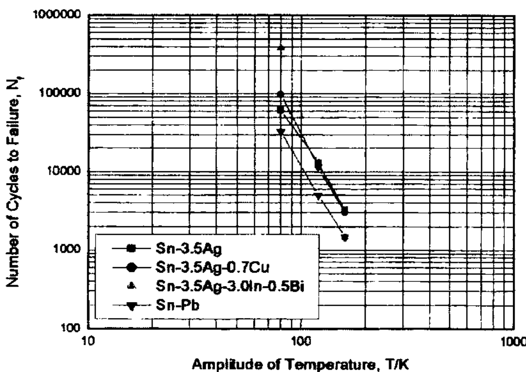

Fig. 6 Log-log graph of ΔT vs N_f

effect of temperature and solder alloys on the fatigue. In this case, the elastic strain was ignored to observe only the effect of low cycle fatigue due to the plastic strain. Logarithm representation of the result is shown in Fig. 6 where the thermal fatigue life is almost linear for four different solder alloys and their temperatures. Thermal fatigue lifes of four different solder alloys show an increasing order: as Sn-3.5Ag-3In-0.5Bi > Sn-3.5Ag-0.7Cu > Sn-3.5Ag > Sn-37Pb at the low temperature range, and Sn-3.5Ag > Sn-3.5Ag-0.7 Cu > Sn-37Pb > Sn-3.5Ag-3In-0.5Bi at the high temperature range. As the amplitude of temperature was increased, Sn-3.5Ag showed the longest fatigue life while Sn-Ag-In-Bi showed the shortest life. This can be interpreted that the properties of In and Bi (Yao et al. 1999 ; Amagai 1999 ; Habu 1999) which has high stiffness at low temperature between 383K~413K but has low stiffness at higher temperature.

3.3 Dimensionless variable, γ

Figure 6 shows the relationship between temperature and number of cycles to failure in the solder joint. It is possible to observe linearity of thermal fatigue life in the solder joint. However, due to the temperature change and the average temperature of thermal cycling on the thermal fatigue life, temperature change and average temperature cannot be ignored. A dimensionless variable γ was introduced to consider the effects of melting point, the average temperature and standard ambient temperature.

$$\gamma = (\Delta T * T_{mean}) / (1/2 * T_m * T_0) \quad (5)$$

where

ΔT(K) : Temperature range,
T_{mean}(K) : Average temperature,
T_m(K) : Melting point,
T_0(K) : Standard ambient temperature

Figure 7 shows the relationship between number of cycles to failure life expressed in log N_f and dimensionless variable log γ.

$$N_f = 10^{\log A + \beta * \log \gamma} \quad (6)$$

$$N_f = A * (\gamma)^{\beta} \quad (7)$$

where

N_f : number of cycles to failure (thermal fatigue life)
A : calculated fatigue material constant,
β : calculated fatigue material exponent

The trend of thermal fatigue life of the solder joint for different operational conditions and melting points can be understood using Fig. 6.

Copyright (C) 2003 NuriMedia Co., Ltd.

Table 3 Calculated fatigue constant of various solder with γ

	Sn-Pb	Sn-Ag	Sn-Ag-Cu	Sn-Ag-In-Bi
log A	2.492	2.774	2.565	1.716
β	−4.967	−4.660	−5.561	−8.887

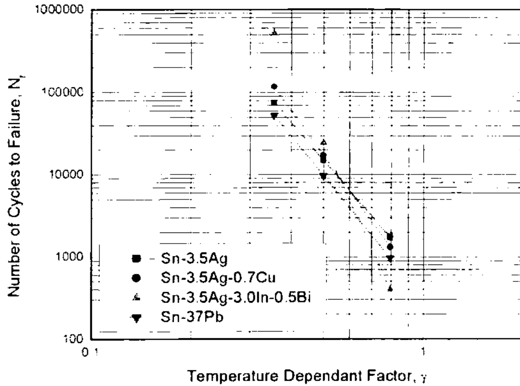

Fig. 7 Log-log graph of ΔT vs N_f

The Eqs. (6) and (7) and Table 3 can be derived from the data shown in Fig. 7.

Thermal fatigue life obtained for different temperatures and dimensionless variable γ are presented in Table 4. Figure 8 shows the number of cycles to failure data obtained by using γ and FEA. As shown in the Fig. 8, the result obtained from γ agrees with FEA result. The Eq. (5) can be used to understand the physical meaning of γ for the thermal fatigue life estimation. When all variables are set to be constant, γ increases as $1/2T_m$ decreases or T_{mean} increases. On the other hand, it is observed that the γ variable increases as the ΔT increases while other variables fixed. At the same time, when the solder temperature is increased, the plastic deformation rate becomes larger. The region affected by the high temperature fracture behavior also becomes wider during the total temperature cycling.

Although there are some differences according to the material and its mean temperature, the ratio of the elastic deformation to the total deformation generated on the concerned part becomes larger. Therefore, the influence of elastic deformation cannot be ignored in estimating the fatigue life.

However, fatigue fracture, which is generated by elastic or elastic-plastic deformation for most materials, lies in the domain of high cycle fatigue. The thermal fatigue life by high cycle fatigue becomes larger as compared to that by low cycle fatigue, which is the main topic in this paper.

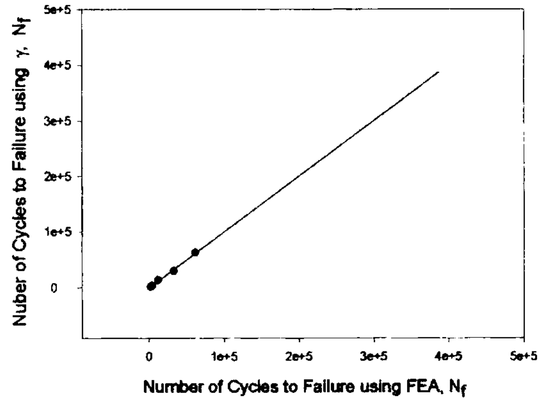

Fig. 8 Thermal fatigue life with γ vs FEA

In other words, the γ can be considered as an important parameter in determining severeness of the environment of solder application.

Applying this parameter for the materials considered in this study and comparing with the computed results, it is found that the solder alloys with larger γ such as the Sn-37Pb have longer fatigue life as compared to the Sn-Ag solder alloys that have smaller γ at the same temperature level. Within the temperature range between 293K and 373K where γ is very small, the effect of the elastic deformation cannot be ignored. These results coincide with earlier discussion.

However, Eq. (6) cannot be used for estimating the thermal fatigue life when the temperature is low enough where the elastic strain cannot be ignored. In this case, the combined effects of low and high cycle fatigue should be used for the life estimation. By examining the relation between the thermal fatigue life and the shape of solder joint using the data in Table 2, it was found that the longest life was obtained when the solder ball was formed 50 degree angle with a line perpendicular to the package base. When the upper part of the solder joint, where stress concentration usually occurs, became more concave than 50-degree angle, the stress was well distributed. The effect of the solder shape on life was more evident for

Copyright (C) 2003 NuriMedia Co., Ltd.

Table 4 γ and number of cycles to failure of four different solder alloys

T(K)	Sn-37Pb		Sn-3.5Ag		Sn-3.5Ag-0.7Cu		Sn-3.5Ag-3In-0.5Bi	
	γ	N_f	γ	N_f	γ	N_f	γ	N_f
293~373	0.399	29782	0.368	62682	0.371	91140	0.371	349119
273~373	0.562	5433	0.519	12627	0.523	13502	0.523	16507
253~393	0.750	1295	0.692	3304	0.698	2712	0.698	1269

solders of the light material. Since the effect of the solder shape on the fatigue life is significant, more systematic research on practical life for different solder shapes is required.

The results obtained by FEA can be used to select the optimum solder type and shape, which assures the acceptable thermal fatigue life at various operation conditions. In this research, effects of micro crack at bonded interface due to the metallurgical structure change caused during the process and operation conditions were not considered. The effect of creep deformation, which was not well understood for some materials, was also ignored. Therefore, the result obtained from this research may be applied directly to the solder alloys at a certain temperature range where elastic strain cannot be ignored. In order to find more reliable thermal fatigue life estimation, extensive experiments at various conditions are needed to interpret the effects of the shape and material on the fatigue life.

4. Conclusions

The thermal fatigue life of μBGA joint using different solder alloys and various shapes was investigated by FEA. The conclusions of this study are summarized as followings.

(1) Sn-3.5Ag-0.75Cu showed higher strength than Sn-37Pb by 0.38N at the shear stress test. Sn-2.0Ag-0.5Cu-2.0Bi showed higher strength than Sn-37Pb by 4.14N

(2) Sn-2.0Ag-0.5Cu-2.0Bi showed higher shear strength than Sn-37Pb at initial bonding stress and overall aging condtion.

(3) The thermal fatigue life equation was derived using the dimensionless variable γ obtained from ΔT, T_m and T_{mean} for life estimation of μBGA. The results with γ showed a good agreement with the FEA results.

(4) It was found that Sn-3.5Ag solder alloys showed better thermal fatigue life than Sn-37Pb over the whole temperature range considered. At low temperature range from 293K to 373K, Sn-3.5Ag-3In-0.5Bi showed the best fatigue life. In the temperature range from 233K to 393K, the Sn-3.5Ag showed relatively better fatigue life.

(5) The longest fatigue life can be obtained when the shape of solder joint makes 50 degree to a line perpendicular to package base. This means that the thermal fatigue life of solder joint depends on the local shape of the joint where fracture occurs. It is also observed that the rate of fracture depends on compositions of the solder alloys.

Acknowledgment

This study was supported by the Korea Science and Engineering Foundation(R01-2000-00227)

References

Amagai, M., 1999, "Characterization of Chip Scale Packaging Materials," *Microelectronics & Reliability*, Vol. 39, pp. 1365~1377.

Coffin, L. F., Jr. and Schenectady. N. Y., 1954, "A Study of the Effect of Cyclic Thermal Stress on a Ductile Metal," *Transactions of the ASME*, Vol. 76, pp. 932~950.

Engelmeier, W., 1983, "Fatigue Life of Leadless Chip Carrier Solder Joints During Power Cycling," *IEEE Transactions on Components, Hybrids and Manufacturing Technology*, Vol CHMT-6, No. 3, pp. 232~237.

Habu, K., 1999, "Development of New Pb-free Solder Alloy of Sn-Ag-Bi System," *Proceeding of the 1999 IEEE International Symposium on*

Copyright (C) 2003 NuriMedia Co., Ltd.

Electronics and the Environment, pp. 21~24.

Kariya, Y., Kagawa, H. and Otsuka, M., 1998, "Effect of Strain Rate, Hold Time and Third Element on the Fatigue Damage of Sn-3.5mass% Ag Alloy," *Microjoining and Assembly Technology in Electronics 98*, pp. 259~264.

Lau, John H. and Pao, Yi-Hsin, 1998, *Solder Joint Reliability of BGA, CSP, Flip Chip and Fine Pithch SMT Assemblies*, McGraw-Hill, p. 118.

Lau, John H., Suresh Golwalkar and Steve Erasmus, 1993, "Advatages and Disadvantages of TSOP with Copper Gull-Wing Leads," *Advanced in Electronic Packaging ASME*, EEP-Vol. 4-2, pp. 1119~1126.

Lee, W. W., Nguyen, L. T. and Selvaduray, G. S., 2000, "Solder Joint Fatigue Models : Review and Applicability to Chip Scale Package," *Microelectronics & Reliability*, Vol. 40, pp. 231~244.

Maeda, K., 1999, "Creep Effects on Solder Fatigue and Life time Prediction," *Microjoining* and Assembly Technology in Electronics '99, pp. 57~62.

Oguchi, Y., Kariya, Y. and Otsuka, M., 1998, "Shear Fatigue Characteristics of Sn-Ag-Bi, Sn-Ag-Cu and Sn-Ag-In Solder Joint," *Microjoining* and Assembly Technology in Electronics 98, pp. 253~258.

Partridge, J. and Boysan, P., 1998, "Influence of Process Variables on the Reliability of Micro BGA package Assemblies," *IEEE*, pp. 451~457.

Robert Darveaux, 1995, "Optimizing the Reliability of Thin Small Outline Package (TSOP) Solder Joints," *Advanced in Electronic Packaging ASME*, EEP-Vol. 10-2, pp. 675~685.

Shin. Y. E. and Kim. J. M., 1999, "A Study on the Life Prediction and Quality Improvement of Solder Joint in IC Package," *Journal of KWS*, Vol. 17, No. 1, pp. 124~132.

Yao, Q. and Qu, J., 1999, "Three-Dimensional Versus Two Dimensional Finite Element Modeling of Flip-Chip Packages," *Transactions of the ASME*, Vol. 121, pp. 196~201.

Yao, Q., Qu, J. and Wu, S. X., 1999, "Estimate the Thermomechanical Fatigue Life of Two Chip Scale Packages," *IEEE Proceedings of the 49th Electronic Components & Technology Conference*, pp. 797~802.

Copyright (C) 2003 NuriMedia Co., Ltd.